Open Access Journal

Journal of Power Technologies 96 (2) (2016) 124–136

journal homepage:papers.itc.pw.edu.pl

Modeling and Lyapunov-Designed based on Adaptive Gain Sliding Mode Control for Wind Turbines

Kamel Djamel Eddine Kerrouche[a,*], Abdelkader Mezouar[a], Larbi Boumediene[a], Alex Van Den Bossche[b]

[a] *Electro-technical Engineering Lab, Faculty of Technology, Tahar Moulay University, 20 000 Saida, Algeria;*
[b] *Electrical Energy LAB EELAB, Technologiepark 913 B 9052 Zwijnaarde, Ghent, Belgium;*

Abstract

In this paper, modeling and the Lyapunov-designed control approach are studied for the Wind Energy Conversion Systems (WECS). The objective of this study is to ensure the maximum energy production of a WECS while reducing the mechanical stress on the shafts (turbine and generator). Furthermore, the proposed control strategy aims to optimize the wind energy captured by the wind turbine operating under rating wind speed, using an Adaptive Gain Sliding Mode Control (AG-SMC). The adaptation for the sliding gain and the torque estimation are carried out using the sliding surface as an improved solution that handles the conventional sliding mode control. Furthermore, the resultant WECS control policy is relatively simple, meaning the online computational cost and time are considerably reduced. Time-domain simulation studies are performed to discuss the effectiveness of the proposed control strategy.

Keywords: Wind turbine, Maximum power point tracking, Proportional integral controller, Adaptive sliding mode control,

1. Introduction

The use of fossil fuels in conventional power plants raises environmental concerns, leading investors to turn to renewable resources of energy. In recent years wind power generation has become the most extensively utilized new power generation source in the world [1].

Governments are attracted by Wind Energy Conversion Systems (WECS) because of their sustainability, simple structure, easy maintenance and management. Wind energy is playing a main role in the effort to increase the share of renewable energy sources in the world energy system, helping to meet global energy demand, offering the best opportunity to unlock a new era of environmental protection [2, 3]. The international market of wind energy is expanding, with an average global annual growth rate of 24% for the period 2002-2006, thereby driving technological competition in this area [4, 5].

Wind turbines based on variable-speed operation have been used for many reasons. Among currently available WECS, variable-speed wind turbines are steadily growing their market share, since changes in wind speed are followed by controlling the shaft speed, which allows the turbine to function at its maximum power coefficient over a wide range of wind speeds [6–9]. If the controllers in WECS perform poorly, the quality and volume of the generated power can be affected. Some [10, 11] propose fuzzy logic control to enhance the performance of WECS in terms of reference tracking and sensitivity to variations. In [12], a comparative study is done between polynomial RST and linear quadratic Gaussian theories with varied wind turbine system parameters. Hybrid fuzzy sliding mode control is performed in [13]. In [9] the drawbacks of conventional wind generator control based on PID controllers are overcome by using model reference adaptive and neuro-fuzzy controllers. One of the most important problems involved in developing WECS is related to the insertion of new robust control strategies, based on low computational time and cost algorithms capable of optimizing the efficiency of the system while decreasing structural loading. Sliding mode control has great significance and has witnessed rapid evolution in industrial applications, proving their agility in many aspects.

This paper can be seen as a continuation of the above-mentioned works. First a detailed model for representation of WECS dynamics simulations is described. Then, this study focuses attention on improving a method to allow better performances of the whole system in question, using Lyapunov theory. The control objective is to follow the variable speed characteristics, which makes it possible to search for maximum power conversion operation of the turbine below the

*Corresponding author
Email address: kerrouche20@yahoo.fr (Kamel Djamel Eddine Kerrouche)

rated wind speed. Instead of the conventional classical PI controller [10, 11], a sliding mode controller based on adaptive gain is used in this work, as an effective solution for power conversion optimization while reducing mechanical fatigue and output chattering on the drive train. The main contribution of this study is the application of the adaptive sliding mode control technique to the maximization of power with two different wind speed models.

This paper is organized as follows: at first, the wind speed profile is modeled. Then, entire system model under study is presented. The control structure based on MPPT control strategy with the proposed design of Adaptive SMC is applied to the WECS. Finally, some results of simulations are done with a view to comparing the two controllers: PI and adaptive SMC in MPPT responses. A short conclusion then follows.

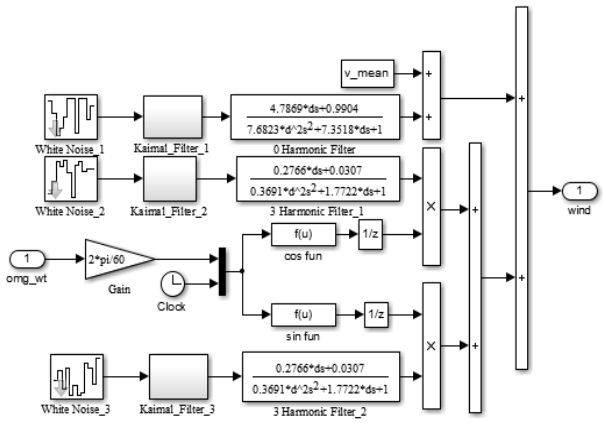

Figure 1: FAST Simulink implementation of wind speed model

2. Wind Speed Modeling

Wind speed generally has complex random variations, both deterministic effects (mean wind, tower shadow) and stochastic fluctuations over time due to turbulence. In this paper, the deterministic and stochastic components are superimposed to form the following wind speed model [14]:

$$V(t) = V_0 + \sum_{i=1}^{n} A_i \sin(\omega_i t + \varphi_i) \tag{1}$$

where: V_0, A_i, ω_i and φ_i are, respectively, the mean component, magnitude, pulsation and initial phase of each turbulence.

As part of this paper, we are interested only in very localized wind: The wind on the area swept by the rotor for a few seconds. In addition, to take into account the turbulent nature of wind, stochastic models are also used. The turbulence spectrum endorsed the distribution of turbulent fluctuations energy, whose integral is determined by the intensity of the turbulence. Turbulence intensity is the following report:

$I = \frac{\sigma}{V_0}$ with the variance $\sigma^2 = \frac{1}{T}\int_0^T V(t)\, dt$

A Gaussian process can generate a turbulent wind distribution. Therefore, the spectrum of Von Karman and one spectrum of Kaimal are the two models used, respecting the standards set by the International Electrotechnical Commission (IEC / IEC) [15].

Von Karman spectrum: $\phi(\omega) = \frac{K}{\left(1+(T\omega)^2\right)^{\frac{5}{6}}}$

Kaimal spectrum: $\phi(\omega) = \frac{K}{|1+T\omega|^{\frac{5}{3}}}$

where: K is a parameter related to the variance T, which determines the bandwidth of turbulence. FAST simulator of the American Laboratory NREL considers these issues and is described in [16]. Indeed, this concept will be used in the modeling equations of the turbine, which will be determined later in this paper. These equations allow us to calculate the average torque actually produced by the turbine. The Danish Riso National Laboratory developed the wind model based Kaimal filter. This model is implemented in Matlab/Simulink, as shown in Fig. 1.

3. Wind Turbine Modeling

The wind turbine extracts the available energy from the wind and converts it into aerodynamic power. The aerodynamic power is produced from the wind power by a C_p factor called power coefficient or Betz's factor, as [14]:

$$P_{aer} = \frac{1}{2} C_p(\lambda,\beta)\rho S V^3 \tag{2}$$

whereρ is the air density, S is the surface where the aerodynamic power can be obtained and V is the wind velocity.

Based on the modeling turbine characteristics, the power coefficient C_p can be represented by the following expression [3]:

$$C_p(\lambda,\beta) = c_1\left(\frac{c_2}{\lambda_i} - c_3\,\beta - c_4\right) e^{\frac{c_5}{\lambda_i}} + c_6\lambda \tag{3}$$

where $\frac{1}{\lambda_i} = \frac{1}{\lambda+0.08\beta} - \frac{0.035}{\beta^3+1}$

The power coefficient C_p depends on the ratio λ and the pitch angle β. This ratio is between linear speed at the tip of the blades and the wind speed:

$$\lambda = \frac{\Omega_t R}{V} \tag{4}$$

where Ω_t is the turbine shaft speed.

Fig. 2 shows the relation between C_p, β and λ. As can be seen from this figure, the pitch angle $\beta = -2°$ normally captures more power with higher C_p, but it has greater difficulty with starting and may be noisier with more peaked power coefficient.

Likewise, the blade angle can resonate and become unstable. To optimize the generated power, it is therefore appropriate for the generator to have power or torque characteristics that follow the maximum $C_{p\max}$ line with the pitch an-

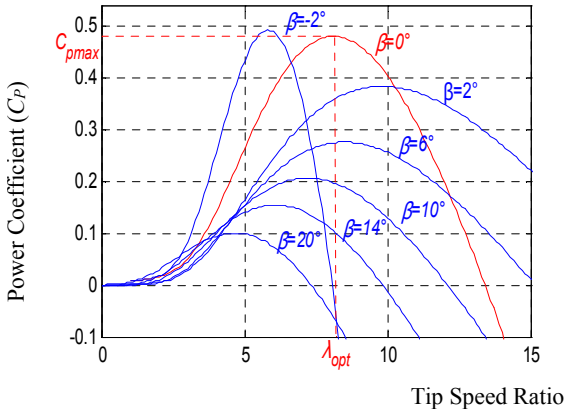

Figure 2: Power coefficient variation against tip speed ratio and pitch angle

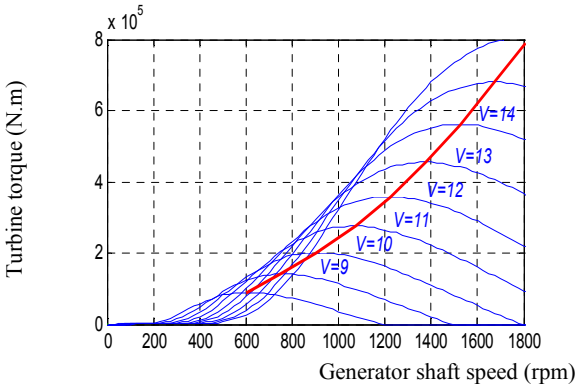

Figure 3: The turbine torque versus the generator shaft speed characteristic at different wind speed

gle $\beta = 0°$. The turbine torque is the ratio of the aerodynamic power to the turbine shaft speed:

$$T_{aer} = \frac{P_{aer}}{\Omega_t} \tag{5}$$

The derivation of the mathematical two-mass model from a three-mass model is presented in [17] and a more detailed demonstration in [15]. In [18] a two-mass drive train model is used, which is significant for short-term voltage stability studies. Considering the assumption of this model, the torque and shaft speed of generator are given by:

$$\begin{cases} T_g = \frac{T_{aer}}{G} \\ \Omega_g = G\,\Omega_t \end{cases} \tag{6}$$

where Ω_g, T_g and G are, respectively, the generator shaft speed, the generator torque and the gear ratio. Using (6), the resulting mechanical equation of the generator shaft is given as follows [19]:

$$\frac{d\Omega_g}{dt} = \frac{1}{J}\left(T_g - T_{em} - f_v\,\Omega_g\right) \tag{7}$$

where T_{em} is the electromagnetic torque, J is the total moment of inertia and f_v is the coefficient of viscous friction.

Rearranging (2), the aerodynamic power can be described as:

$$P_{aer} = k_t\,(\beta)\,\Omega_t^3 \tag{8}$$

where: $k_t\,(\beta) = \frac{\frac{1}{2} C_p(\beta)\,\rho\,S\,R^3}{\lambda^3}$

An expression for the turbine torque T_{aer} is obtained from the ratio P_{aer}/Ω_t. The turbine torque versus the turbine shaft speed characteristics at different wind speeds is presented in Fig. 3; the geometric locus corresponding to the maximum power points is also depicted in this figure in red bold line.

4. Wind Turbine Control

Many approaches of Maximum Power Point Tracking (MPPT) have been discussed in the literature [15, 19]. Control of the torque (thus power) aims to extract the maximum available power from the wind by adapting the generator shaft speed. To realize this objective, the turbine tip speed ratio should be kept at its optimum value ($\lambda = \lambda_{opt}$) despite wind variations, where the turbine captures the maximum energy from the wind [9]. In [20], the MPPT based on wind speed estimation may provide uncertain values in the case of aerodynamic deviations, such as air density (ρ) discrepancies.

4.1. Sliding Mode Control of the Wind Turbine

Sliding Mode Control (SMC) is a Variable Structure Control (VSC) based on Lyapunov theory. This proposed theory has been described in the works reported in [20, 21].

Supposing the wind turbine model is controllable and observable, the SMC consists of the following three main steps:

1. Selection of the sliding surface.
2. Study of the existence of the reaching condition.
3. Determination of control law.

From (4), the optimal turbine shaft speed is defined as:

$$\Omega_{t,opt} = \frac{\lambda_{opt}\,V}{R} \tag{9}$$

According to the gearbox model, the reference generator shaft speed is:

$$\Omega_g^* = G\,\Omega_{t,opt} \tag{10}$$

Then, the first order tracking error dynamics of the proposed sliding surface is equal to the error between the actual and the reference speed:

$$S\,(\Omega_g) = e(\Omega_g) = \Omega_g - \Omega_g^* \tag{11}$$

From (7), the derivative of sliding surface given in (11) is:

$$\dot{S}\,(\Omega_g) = \frac{1}{J}\left(T_g - T_{em} - f_v\,\Omega_g\right) - \dot{\Omega}_g^* \tag{12}$$

The expression of sliding surface derivative (12) is rewritten as:

$$\dot{S}(\Omega_g) = F + D\,T_{em} \tag{13}$$

where $F = \frac{1}{J}\left(T_g - f_v\,\Omega_g\right) - \dot{\Omega}_g^*$and $D = -\frac{1}{J}$

In order to ensure system stability, Lyapunov function is considered [21]:

$$V = \frac{1}{2}S(\Omega_g)^2 \tag{14}$$

The control law is designed in order to satisfy the condition of the reachability and existence of the sliding mode:

$$\dot{V} = S\left(\Omega_g\right)\dot{S}\left(\Omega_g\right) < 0 \tag{15}$$

The torque control law must ensure the stability condition and the convergence of the system trajectories toward the sliding surface $S(\Omega_g) = 0$, since:

If $S\left(\Omega_g\right) < 0$ and $\dot{S}\left(\Omega_g\right) > 0$, therefore $S\left(\Omega_g\right)$ will increase to zero.

If $S\left(\Omega_g\right) > 0$ and $\dot{S}\left(\Omega_g\right) < 0$, therefore $S\left(\Omega_g\right)$ will decrease to zero.

The third step is to determine the control law. The equivalent control is required to guarantee control of the nominal plant model and the switching part of the control is added to keep the desired performance despite variations in parameters.

The equivalent control is found by letting $\dot{S}(\Omega_g) = 0$, from (13) the following expression is obtained:

$$T_{em,eq} = T_g - f_v\,\Omega_g - J\,\dot{\Omega}_g^* \tag{16}$$

By introducing the switching control, the control law becomes:

$$T_{em}^* = T_g - f_v\,\Omega_g - J\,\dot{\Omega}_g^* + J\,K_{\Omega g}\,sign(S(\Omega_g)) \tag{17}$$

where $K_{\Omega g}$is sliding gain, the function $sign\left(S\left(\Omega_g\right)\right)$ is defined as follows:

$$sign\left(S\left(\Omega_g\right)\right) = \begin{cases} 1 & if \quad S\left(\Omega_g\right) > 0 \\ 0 & if \quad S\left(\Omega_g\right) = 0 \\ -1 & if \quad S\left(\Omega_g\right) < 0 \end{cases} \tag{18}$$

Substituting the control law (17) into the resulting mechanical equation of the generator shaft (7), the dynamics of the closed-loop system are settled as follows:

$$\dot{S}(\Omega_g) = -K_{\Omega g}\,sign\left(S\left(\Omega_g\right)\right) \tag{19}$$

4.2. Adaptive Gain Sliding Mode Control

The adaptation of the time sliding gain $K_{\Omega g}(t)$ is used in order to enhance the system's response. Then, the control law becomes:

$$T_{em}(t) = T_g(t) - f_v\,\Omega_g(t) - J\,\dot{\Omega}_g^*(t) + J\,K_{\Omega g}(t)\;sign\left(S\left(\Omega_g\right)\right) \tag{20}$$

According to [22], the rate of change of the time sliding gain $K_{\Omega g}(t)$ is based on sliding surface $S_{\Omega_g}$and the rate of change of this surface, with respect to the sliding gain, which is determined as follows:

$$\dot{K}_{\Omega g}(t) = -\alpha\,S\left(\Omega_g\right)\frac{\partial}{\partial K_{\Omega g}}\dot{S}(\Omega_g) \tag{21}$$

where $\alpha$is the positive scalar.

Substituting the derivative of the sliding surface from (19), with respect to the sliding gain, into (21), the derivative of the sliding gain becomes:

$$\dot{K}_{\Omega g}(t) = \alpha\,S\left(\Omega_g\right)\;sign\left(S\left(\Omega_g\right)\right) \tag{22}$$

The adaptation of the sliding gain is expressed as follows:

$$K_{\Omega g}(t) = \int \alpha\,S\left(\Omega_g\right)\;sign\left(S\left(\Omega_g\right)\right)\,dt \tag{23}$$

Generator Torque Estimation. In this subsection, the control strategy is based on generator torque estimation, which is considered as unknown by the controller.

The control law (21) has the following expression:

$$T_{em}^*(t) = \hat{T}_g(t) - f_v\,\Omega_g(t) - J\,\dot{\Omega}_g^*(t) + J\,K_{\Omega g}(t)\;sign\left(S\left(\Omega_g\right)\right) \tag{24}$$

where $\hat{T}_g$ is an estimate of the generator torque.

The dynamics of the closed-loop system are established as follows:

$$\dot{S}_{\Omega g} = -K_{\Omega g}\;sign\left(S\left(\Omega_g\right)\right) + \frac{1}{J}\,\tilde{T}_g \tag{25}$$

where $\tilde{T}_g = \hat{T}_g - T_g$ is the generator torque error.

Using the adaptive torque estimator $\hat{T}_g$, the closed loop dynamics (25) are similar to (19). The first-order dynamics of the generator torque error are imposed as:

$$\dot{\tilde{T}}_g + a_0\tilde{T}_g = 0, a_0 > 0 \tag{26}$$

The variation of the dynamics of the electric generator is very fast compared to the generator torque $\dot{T}_g = 0$. This assumption of the neglected generator torque variation will not affect the estimation performance. Using the expression of T_g from (7) and the previous assumption $\dot{T}_g = 0$, the equation (27) is rearranged as:

$$\dot{\hat{T}}_g = a_0\left(T_g - \hat{T}_g\right) = a_0\,\left(f_v\,\Omega_g + J\,\dot{\Omega}_g^* + T_{em}\right) - a_0\,\hat{T}_g \tag{27}$$

Substituting the control law from (20) into (27), the estimated torque becomes:

$$\hat{T}_g(t) = a_0\,J\,S\left(\Omega_g\right) - a_0\,J\int K_{\Omega g}(t)\;sign\left(S\left(\Omega_g\right)\right)\,dt \tag{28}$$

The generation system operated well and achieved the MPPT curve during variation of generator shaft speed. The electromagnetic will be an input for the control loop described in section IV. It should be stated that the present work focuses on MPPT. Accordingly, the AG SMC of the wind turbine is shown in Fig. 4 (second select mode).

This control block also proposes a select mode to choose the operating mode; the first select mode for the MPPT is based on wind speed measurement with a simple anemometer and speed control with a classical PI controller.

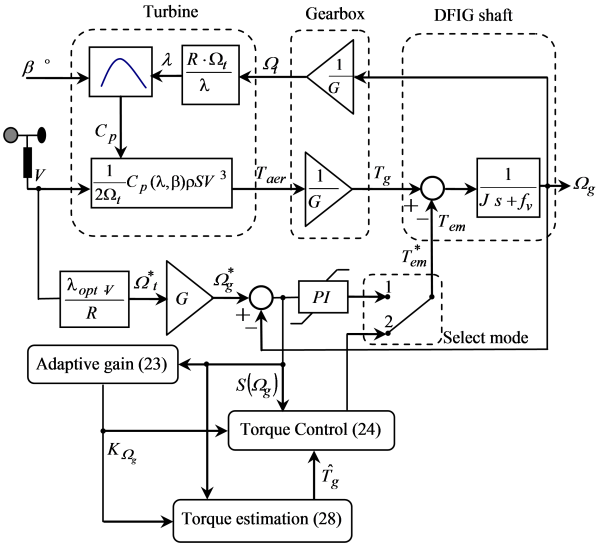

Figure 4: Wind turbine model and control structure

5. Simulation Results and Discussion

In practice, the parameters are never determined according to inequalities. Therefore, the appropriate technique is to adapt the controller parameters during computer simulations. The parameters of the WECS are reported in the Appendix.

All the simulations were elaborated with a fixed-step size of 0.1 m s with a view to digital implementation in future works.

The first wind speed profile used in this simulation based on equation (1) is shown in Fig. 5. Although it is not typically the case in reality, this shape is very frequently used in simulations, as it is simple to use and shows the worst case. In addition, the second wind speed profile based on the FAST model is shown in Fig. 6. The MPPT control is then applied by the conditions given from Fig. 2, the maximum values of power coefficient $C_{p,\max}$ and the optimum speed ratio λ_{opt} for the curve associated to the fixed pitch angle $\beta = 0°$. The pitch angle is maintained at its fixed value, without power limitation below the rated wind speed. The following simulation results are performed to compare the two controllers, namely, the classical PI controller and the proposed Adaptive Gain Sliding Mode Control (AG-SMC) algorithm (see Fig. 4). In order to demonstrate the robustness of the proposed controller, the friction coefficient is varied about 25%, uncertainties in the system are under the influence of a white noise added to the turbine torque. These types of noise can include unmodeled quantities.

Fig. 7 and Fig. 8 show the aerodynamic power obtained by using two different models.

In Fig. 9 and Fig. 10, a zoom about the adaptation of time sliding gain $K_{\Omega g}(t)$ is shown, where its value achieves the optimum rapidly and because of the speed error, a small variation occurs.

It is noticed from Fig. 11 and Fig. 12, that the estimated generator torque tracks closely the real torque for both wind speed profiles. This estimation yields to the amelioration of the speed tracking performance, where the steady state error is reduced in the speed tracking due to the integral action in the structure of the torque estimator.

Fig. 13, Fig. 14, Fig. 15, Fig. 16, Fig. 17 and Fig. 18 show the convergence of the generator shaft speed to its reference speed, which is proportional to the curve of the wind speed profile. It can be seen from these figures that the classical PI controller has important ripples in the tracking speed error. In contrast, the AG-SMC performs very well in terms of the tracking speed error, as shown in Fig. 19 and Fig. 20. Therefore, the proposed control algorithm is able to actively follow the generator shaft speed in quick dynamic changes under system uncertainties; the proposed method is effective for real-time electromagnetic torque control under severe randomly varying wind speed and disturbance rejection.

It can be seen from Fig. 21 and Fig. 22 that the MPPT technique ensures the tracking of the optimum power points, by maintaining the power coefficient around its maximum value $C_{p,\max} \approx 0.479$.

It is also shown from Fig. 23 and Fig. 24 that the tip speed ratio is around its optimum value $\lambda_{opt} \approx 8$. Consequently, from these figures, the smoothness of the proposed AG-SMC is proved, and this is responsible for enhanced mechanical behavior. Taking a a comparative approach, it can be deduced from these simulation results that the oscillations in power coefficient and TSR are responsible for the mechanical stresses under the classical PI controller.

6. Conclusions

In this paper, the modeling and control strategy of a Wind Energy Conversion System (WECS) is presented. The randomly varying wind speeds and modeling uncertainties can affect the WECS' efficiency and lead to drive train mechanical stresses. Hence, the control strategy of the wind turbine is required to guarantee robustness against this impact. Lyapunov designed Sliding Mode Control (SMC) is well adapted, using information from the sliding surface. In addition, the effects of external disturbances, unmodelled quantities and parametric inaccuracies have been tackled by the estimation and injection of generator torque, considered as unknown disturbance, into the control law to compensate these effects. This approach was compared with the classical PI controller and validated by simulation. For some results of simulation, the proposed AG-SMC shows itself to be an improvement on the classical PI controller, demonstrating high robustness, accuracy of tracking the maximum conversion efficiency and ability to reduce mechanical stresses. Therefore, the mechanical working life is extended without significantly increasing the complexity of the control.

Future works are oriented at experimental validation, including discrete time version and sliding mode speed observer.

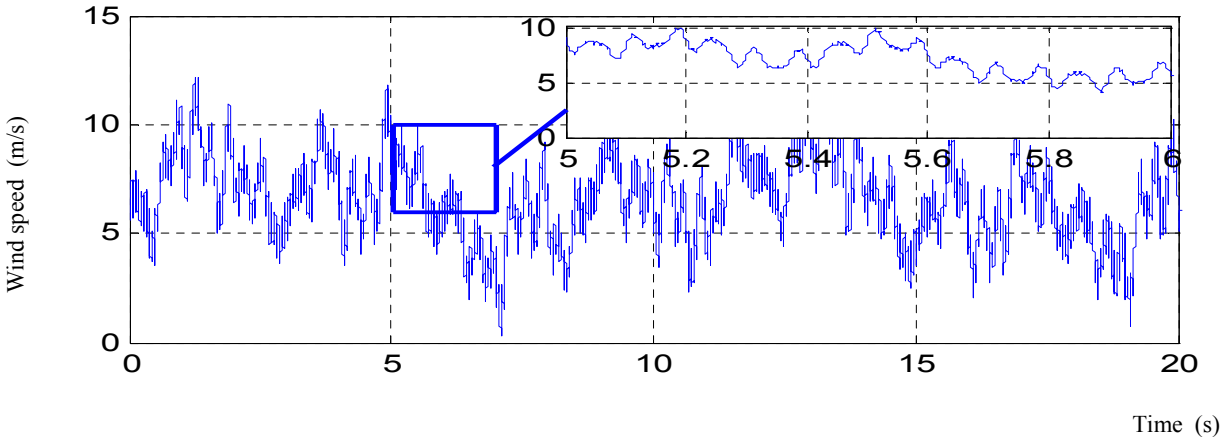

Figure 5: Wind speed profile using equation (1).

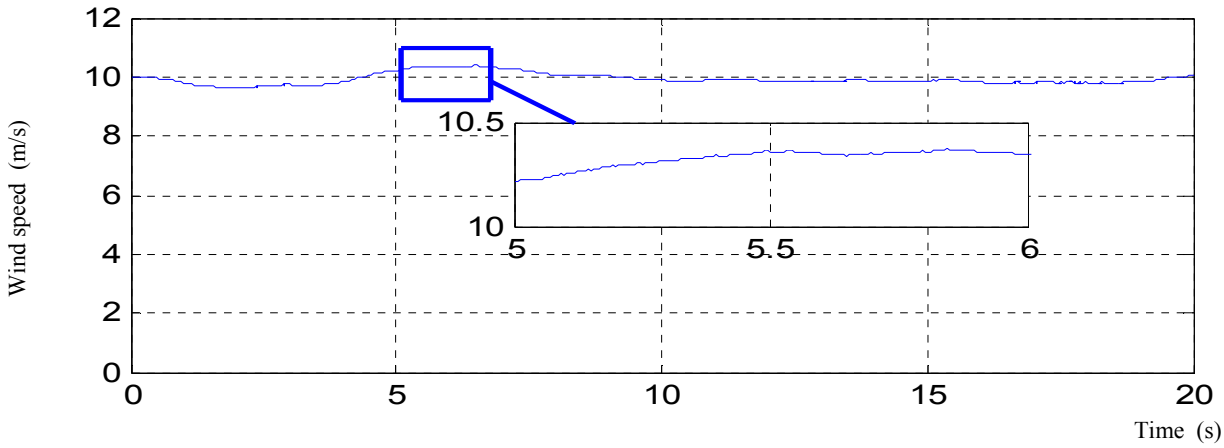

Figure 6: Wind speed profile using FAST model.

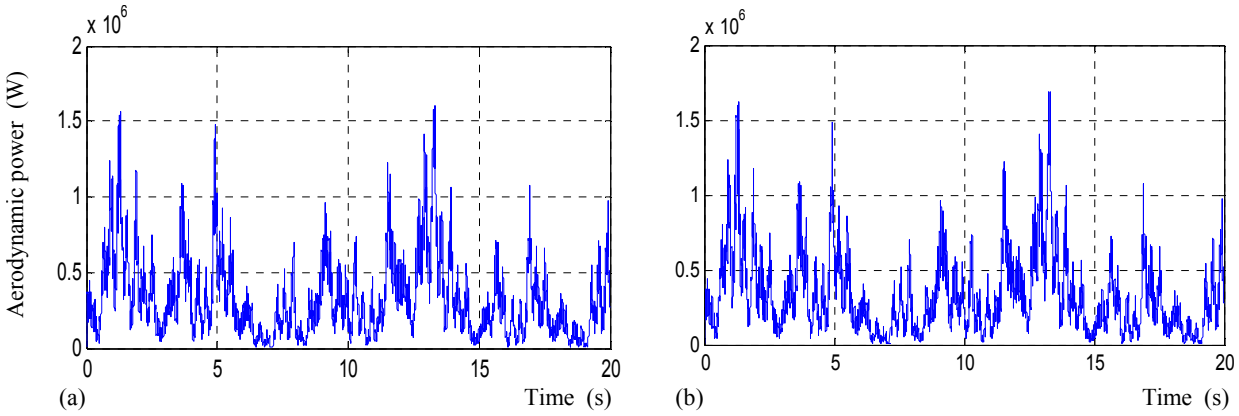

Figure 7: Model based on wind speed using equation (1): (a) Aerodynamic power with PI, (b) Aerodynamic power with AG SMC.

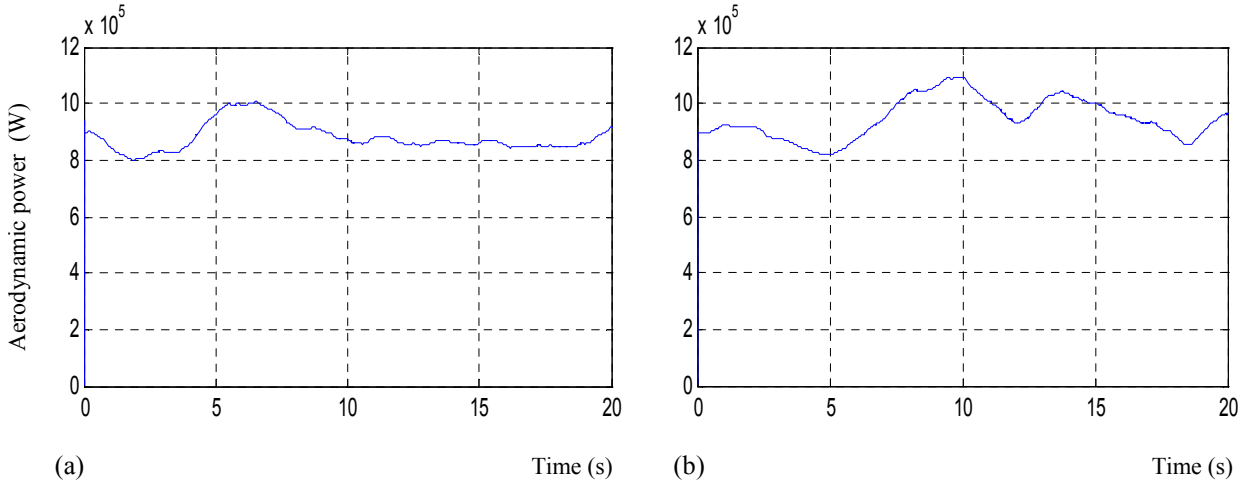

Figure 8: Model based on wind speed using FAST model: (a) Aerodynamic power with PI, (b) Aerodynamic power with AG SMC.

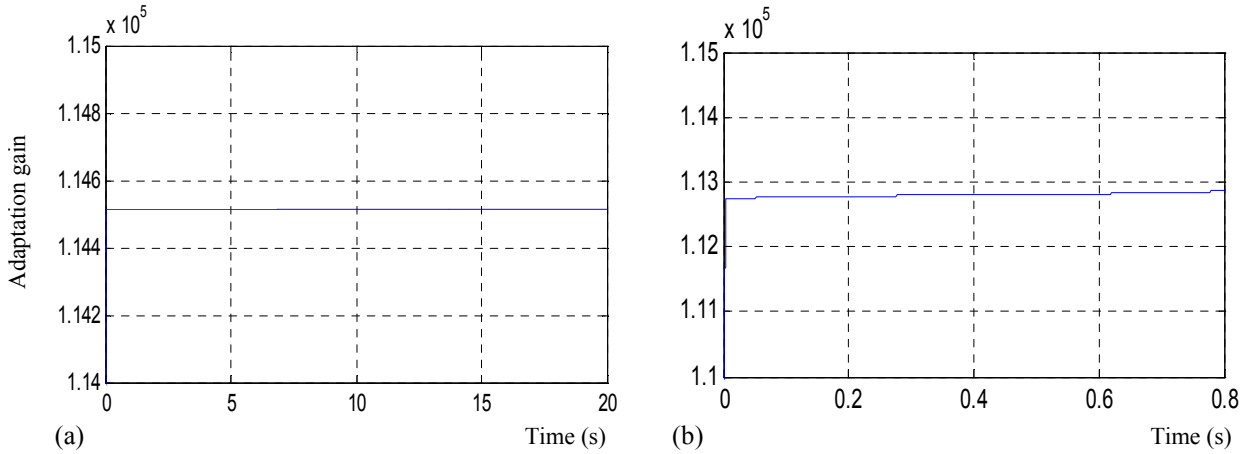

Figure 9: Model based on wind speed using equation (1): (a) (b) Adaptation gain.

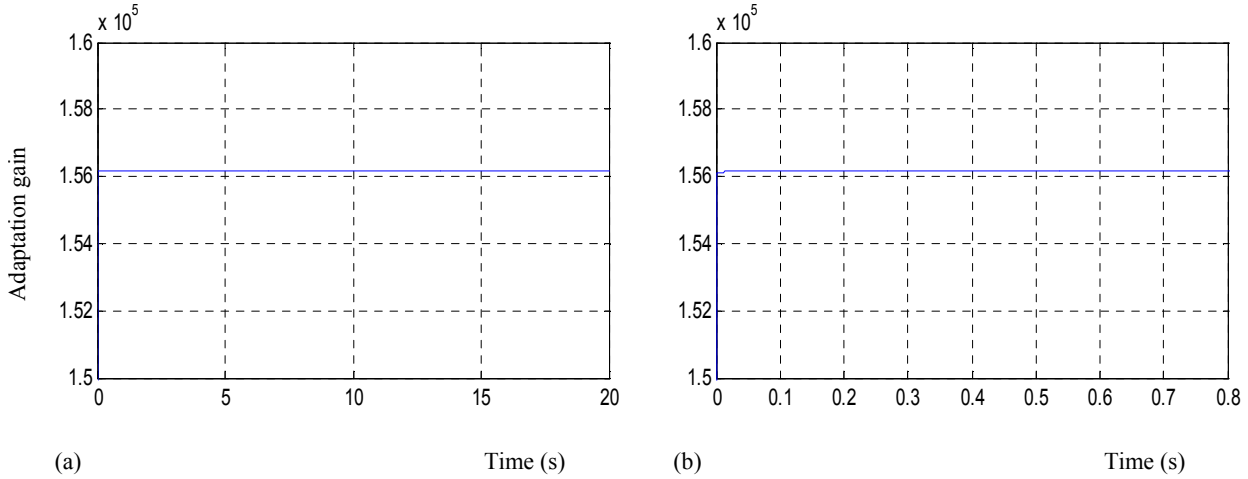

Figure 10: Model based on wind speed using FAST model: (a), (b) Adaptation gain.

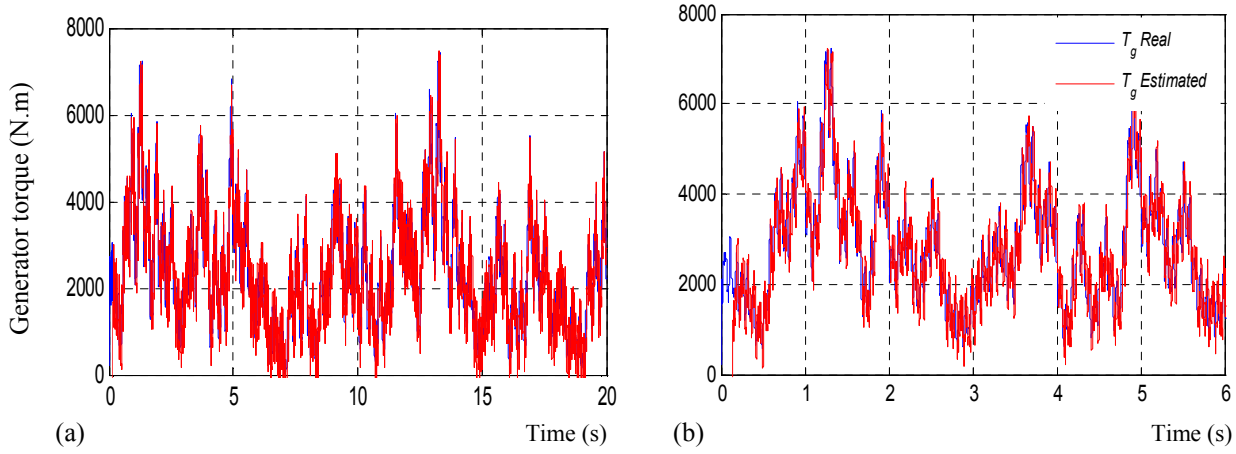

Figure 11: Model based on wind speed using equation (1): (a), (b) Variation of real and estimated generator torque.

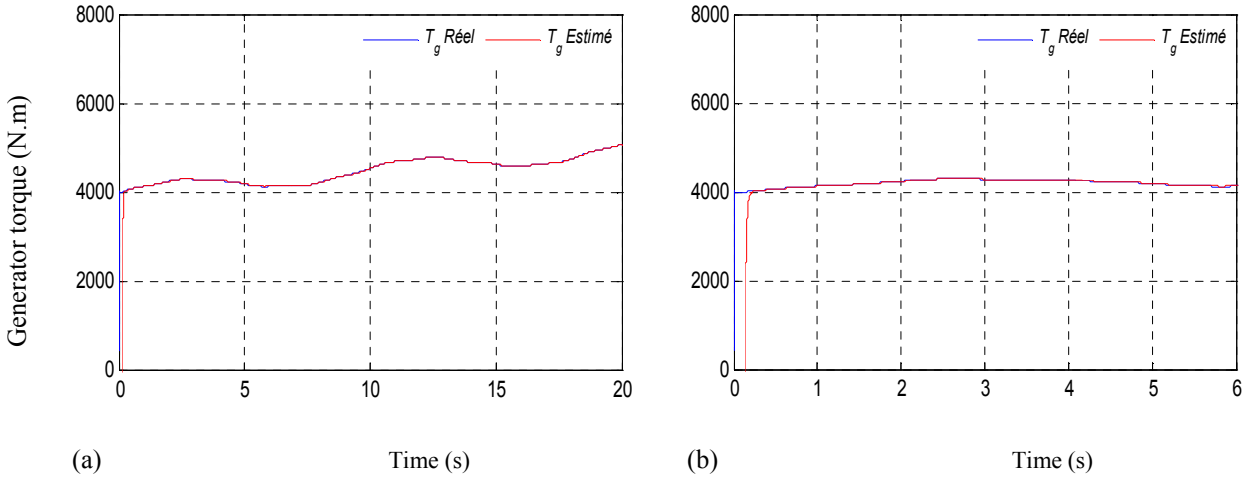

Figure 12: Model based on wind speed using FAST model: (a), (b) Variation of generator real and estimated torque.

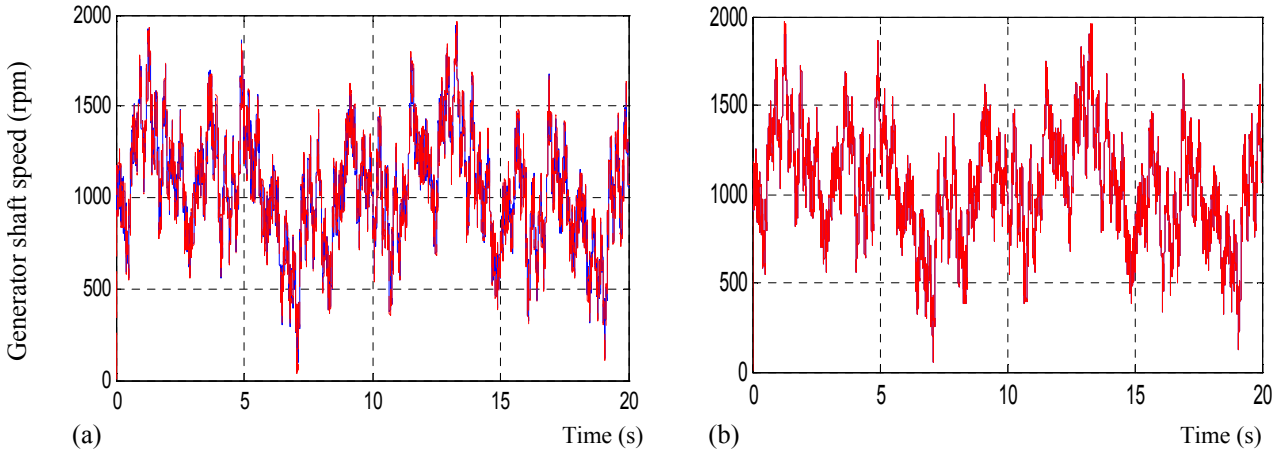

Figure 13: Model based on wind speed using equation (1): (a) Generator shaft speed with PI, (b) Generator shaft speed with AG-SMC.

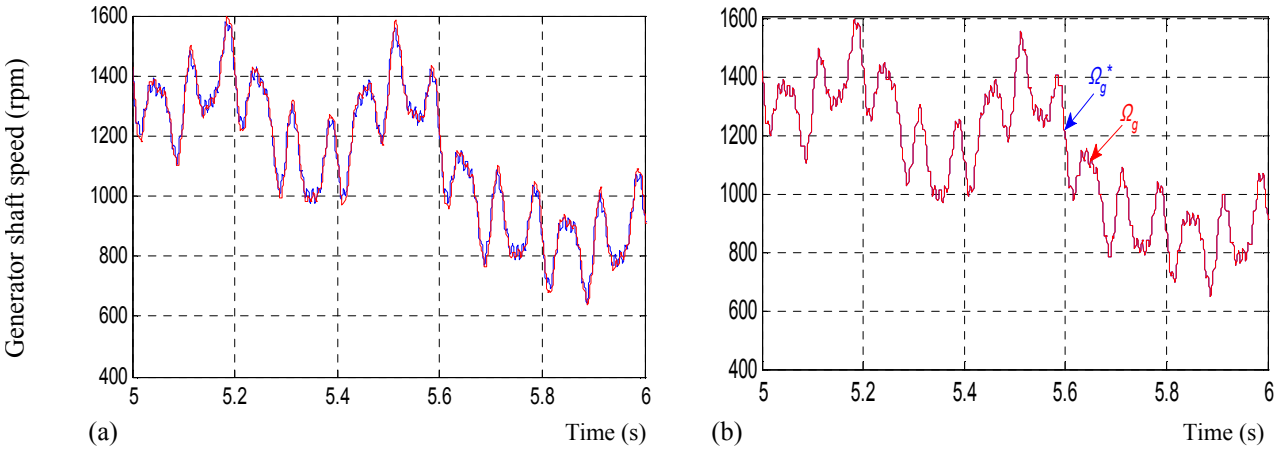

Figure 14: Model based on wind speed using equation (1): (a) Zoom of the generator shaft speed with PI, (b) zoom of the generator shaft speed with AG-SMC.

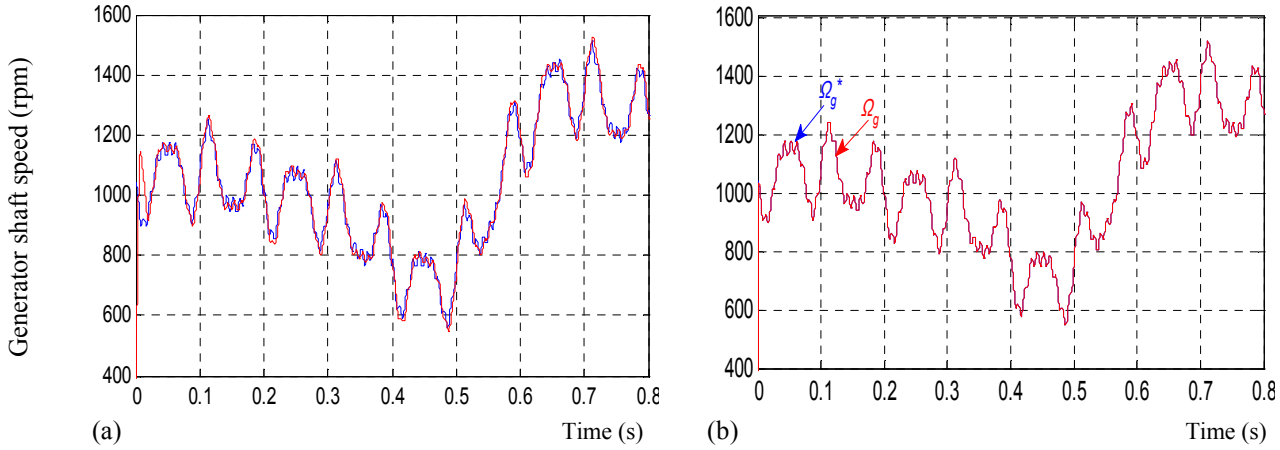

Figure 15: Model based on wind speed using equation (1): (a) Generator shaft speed with PI, (b) Generator shaft speed with AG-SMC.

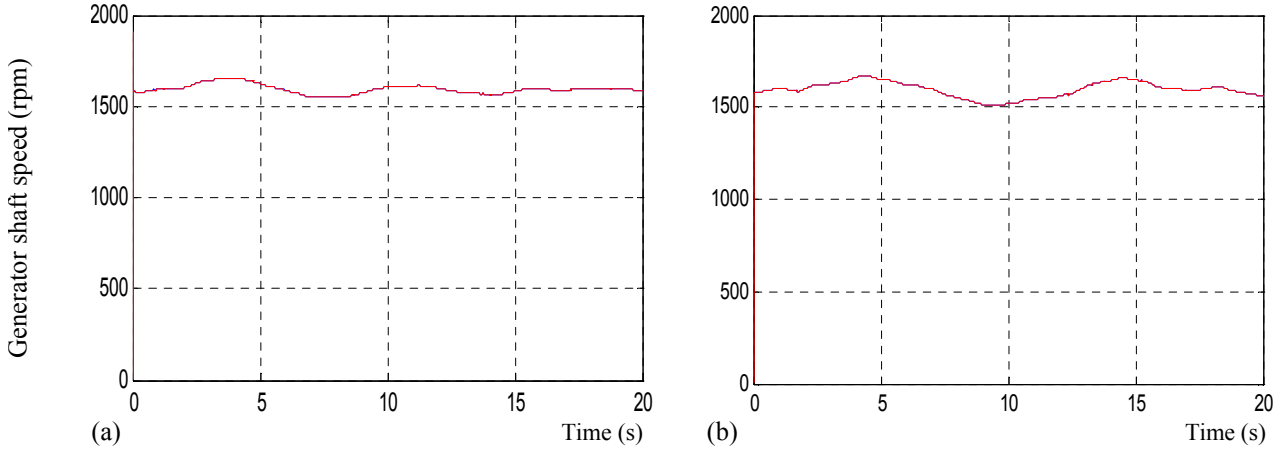

Figure 16: Model based on wind speed using FAST model: (a) Generator shaft speed with PI, (b) Generator shaft speed with AG-SMC.

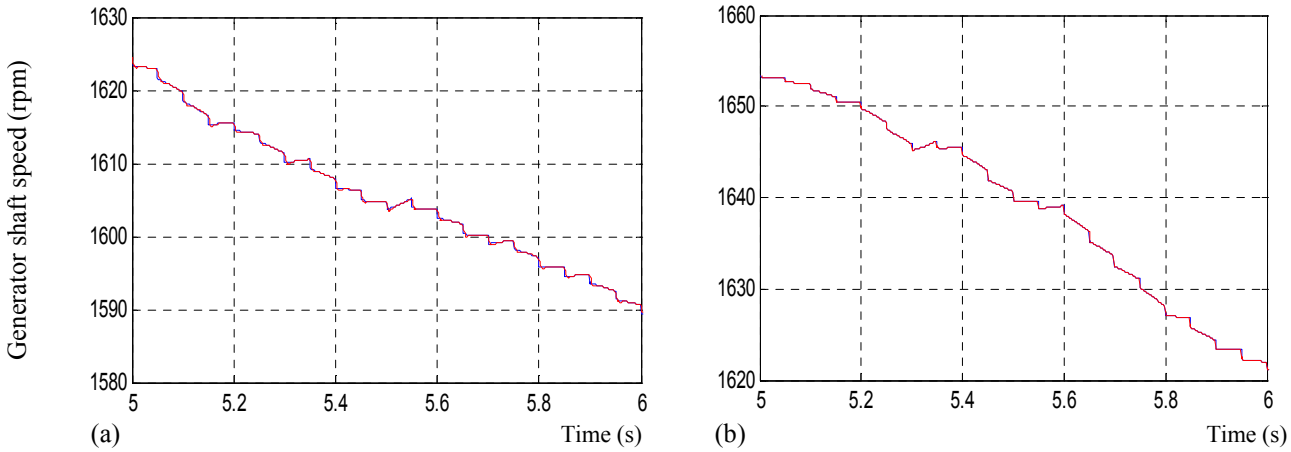

Figure 17: Model based on wind speed using FAST model: (a) Zoom of generator shaft speed with PI, (b) Generator shaft speed with AG-SMC.

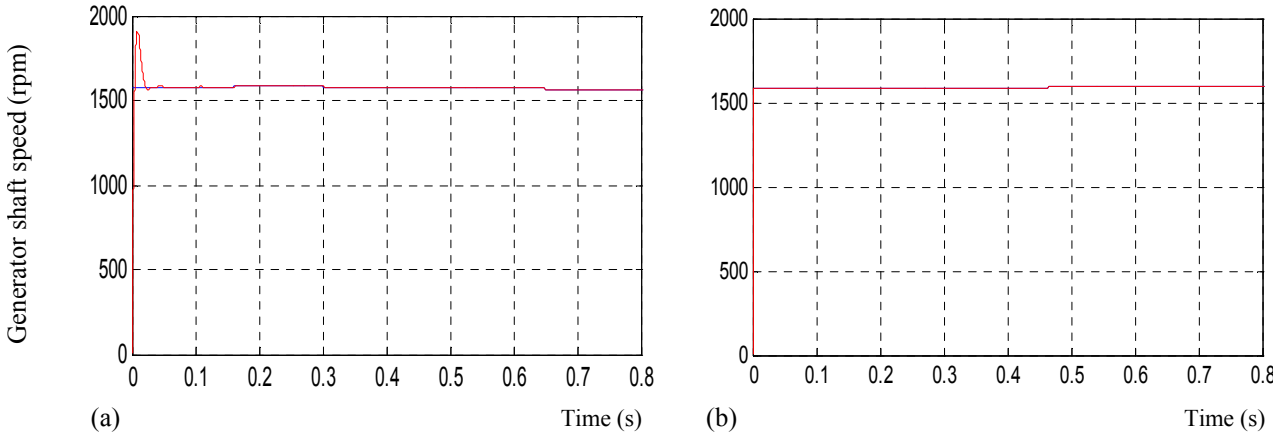

Figure 18: Model based on wind speed using FAST model: (a) Generator shaft speed with PI, (b) Generator shaft speed with AG-SMC.

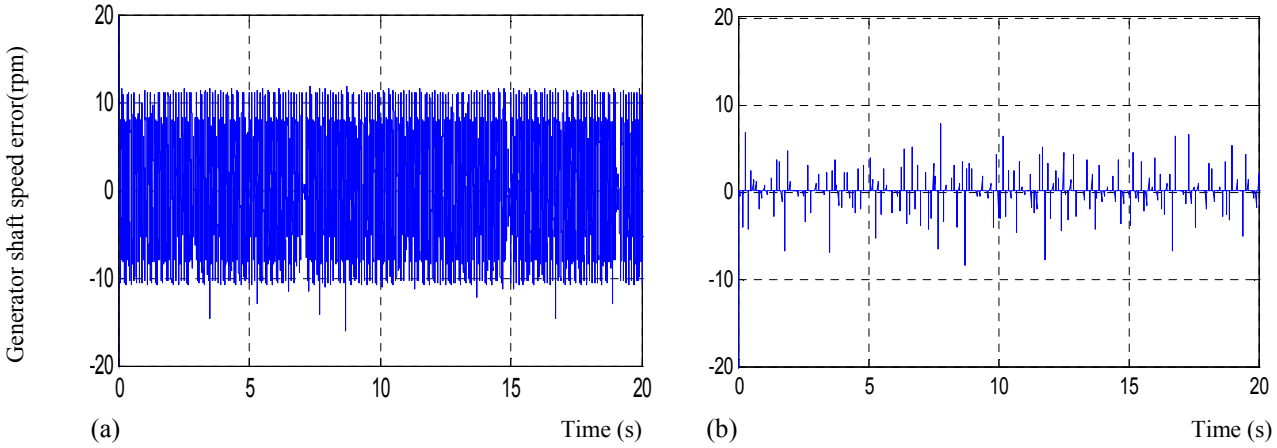

Figure 19: Model based on wind speed using equation (1): (a) Generator shaft speed error with PI, (b) Generator shaft speed with AG-SMC.

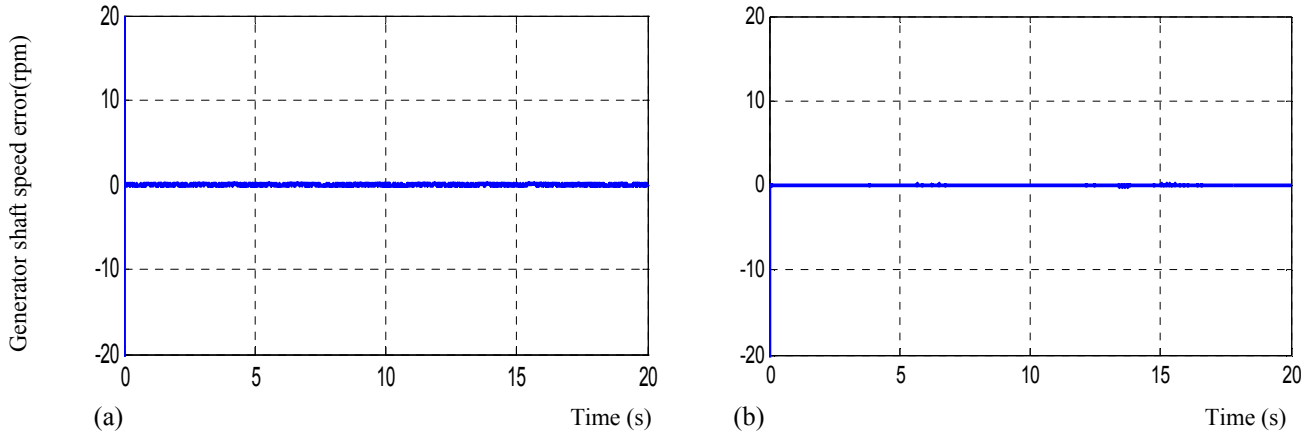

Figure 20: Model based on wind speed using FAST model: (a) Generator shaft speed error with PI, (b) Generator shaft speed with AG-SMC.

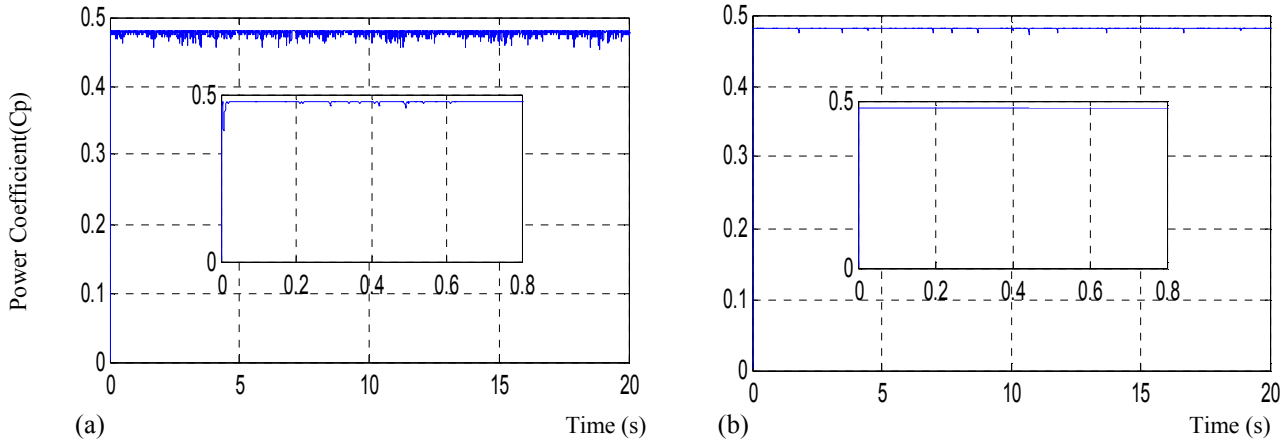

Figure 21: Model based on wind speed using equation (1): (a) Power coefficient with PI, (b) Power coefficient with AG-SMC

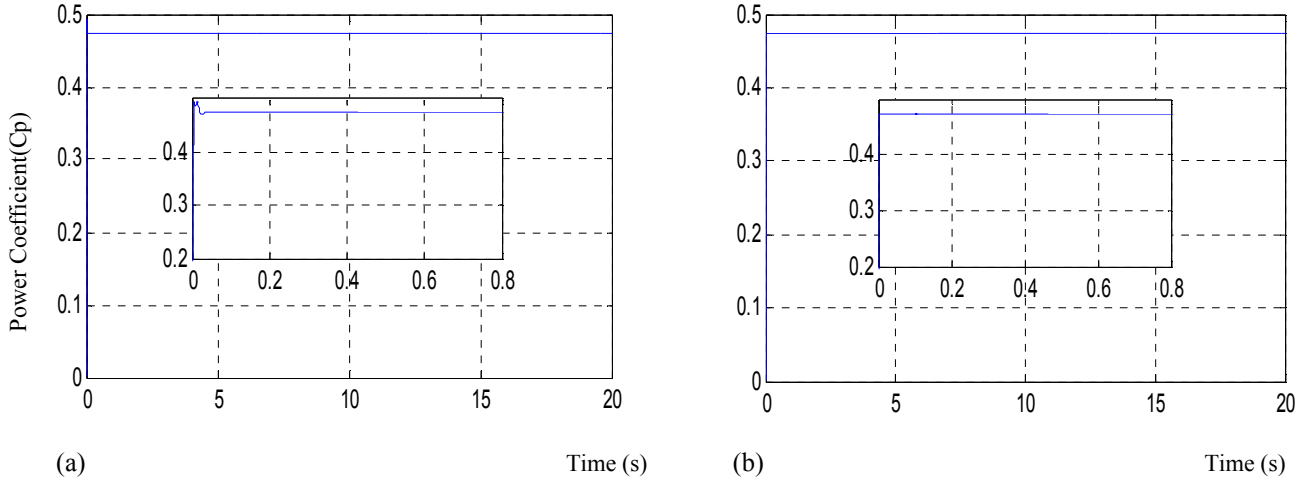

Figure 22: Model based on wind speed using FAST model: (a) Power coefficient with PI, (b) Power coefficient with AG-SMC.

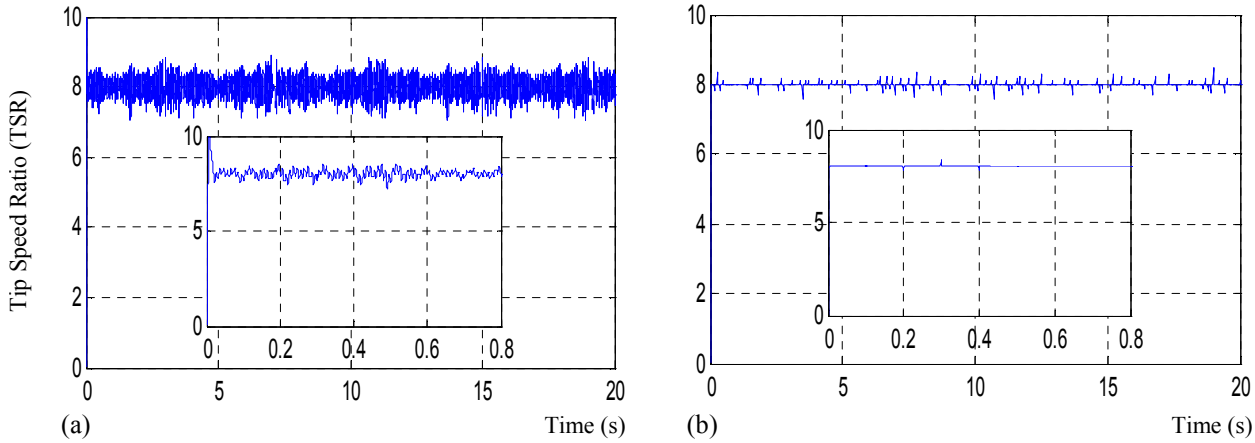

Figure 23: Model based on wind speed using equation (1): (a) Tip speed ratio with PI, (b) Tip speed ratio with AG-SMC.

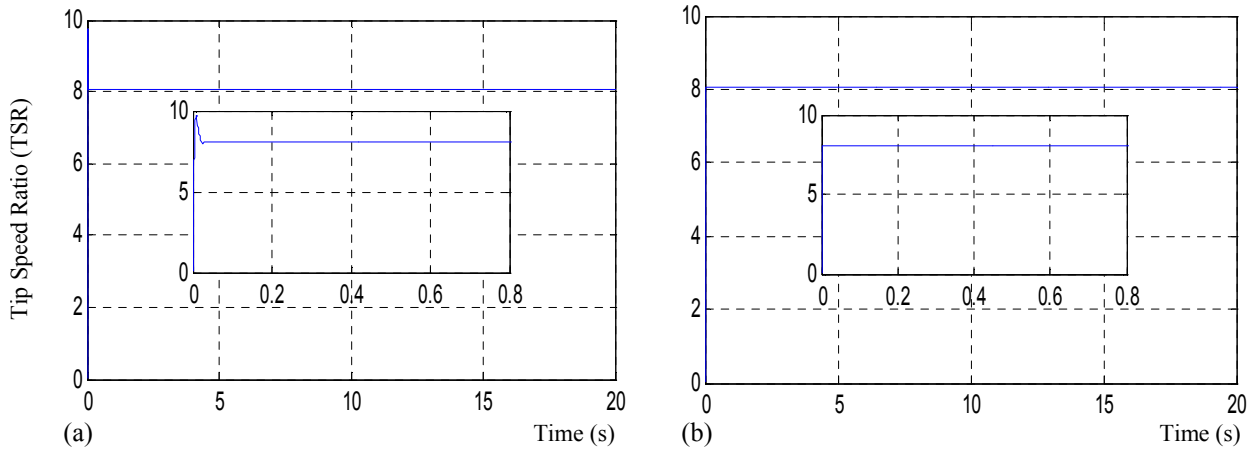

Figure 24: Model based on wind speed using FAST model: (a) Tip speed ratio with PI, (b) Tip speed ratio with AG-SMC.

Acknowledgements

The authors would like to acknowledge the financial support of Algeria's Ministry of Higher Education and Scientific Research, under CNEPRU project: J02036 2014 0003.

Appendix

In this part, simulations are investigated with a 1.5 MW generator wind turbine [23]. The parameters of the turbine are presented below:

Parameters	values
Turbine radius, m	35.25
Gear box ratio	90
Inertia, kg.m^2	1000
Friction factor, kg.m/s	0.0024

The turbine characteristics are:

$$c_1 = 0.5176,\ c_2 = 116,\ c_3 = 0.4,\ c_4 = 5,\ c_5 = 21,\ c_6 = 0.0068.$$

References

[1] M. H. Baloch, J. Wang, G. S. Kaloi, (0043) modeling and controller design for wind energy conversion system based on a cage induction generator using turbulence speed, Journal of Power Technologies.
[2] T. Ackermann, Wind power in power systems, in JG. Slootweg, H. Polinder, W L. Kling, Reduced Order Modeling of Wind Turbines, New York, NY, USA: Wiley (2005) 555–585.
[3] J. Slootweg, H. Polinder, W. Kling, Reduced-order modelling of wind turbines, Wind power in power systems (2005) 555–585.
[4] K. Kerrouche, A. Mezouar, L. Boumedien, The suitable power control of wind energy conversion system based doubly fed induction generator, International Journal of Computer Applications 87 (3).
[5] O. Publishing, I. E. Agency, World energy out look. Paris: Organisation for Economic Cooperation and Development; 2010.
[6] E. W. E. Association, Wind directions-the European wind industry magazine 1 (1) (2012).
[7] A. Nadhir, T. Hiyama, Maximum power point tracking based optimal control wind energy conversion system, in: Advances in Computing, Control and Telecommunication Technologies (ACT), 2010 Second International Conference on, IEEE, 2010, pp. 41–44.
[8] K. Ghedamsi, D. Aouzellag, E. Berkouk, Control of wind generator associated to a flywheel energy storage system, Renewable Energy 33 (9) (2008) 2145–2156.
[9] F. Amrane, A. Chaiba, S. Mekhilef, High performances of grid-connected dfig based on direct power control with fixed switching frequency via mppt strategy using mrac and neuro-fuzzy control, Journal of Power Technologies 96 (1) (2016) 27–39.
[10] V. Calderaro, V. Galdi, A. Piccolo, P. Siano, A fuzzy controller for maximum energy extraction from variable speed wind power generation systems, Electric Power Systems Research 78 (6) (2008) 1109–1118.
[11] V. Galdi, A. Piccolo, P. Siano, Exploiting maximum energy from variable speed wind power generation systems by using an adaptive takagi–sugeno–kang fuzzy model, Energy Conversion and Management 50 (2) (2009) 413–421.
[12] F. Poitiers, T. Bouaouiche, M. Machmoum, Advanced control of a doubly-fed induction generator for wind energy conversion, Electric Power Systems Research 79 (7) (2009) 1085–1096.
[13] A. Kerboua, Hybrid fuzzy sliding mode control of a doubly-fed induction generator speed in wind turbines, Journal of Power Technologies 95 (2) (2015) 126.
[14] K. D.-E. Kerrouche, A. Mezouar, L. Boumediene, K. Belgacem, Modeling and optimum power control based dfig wind energy conversion system, International Review of Electrical Engineering (IREE) 9 (1) (2014) 174–185.
[15] I. Munteanu, A. I. Bratcu, N.-A. Cutululis, E. Ceanga, Optimal control of wind energy systems: towards a global approach, Springer Science & Business Media, 2008.
[16] A. Manjock, Design codes fast and adams for load calculations of onshore wind turbines, 2005, National Renewable Energy Laboratory (NREL): Golden, Colorado, USA.
[17] M. Stiebler, Wind energy systems for electric power generation, Springer Science & Business Media, 2008.
[18] A. Petersson, T. Thiringer, L. Harnefors, T. Petru, Modeling and experimental verification of grid interaction of a dfig wind turbine, Energy Conversion, IEEE Transactions on 20 (4) (2005) 878–886.
[19] S. Abdeddaim, A. Betka, Optimal tracking and robust power control of the dfig wind turbine, International Journal of Electrical Power & Energy Systems 49 (2013) 234–242.
[20] K. Kerrouche, A. Mezouar, L. Boumedien, A simple and efficient maximized power control of dfig variable speed wind turbine, in: Systems and Control (ICSC), 2013 3rd International Conference on, IEEE, 2013, pp. 894–899.
[21] V. I. Utkin, Sliding Modes in Optimization and Control. New York: Springer-Verlag, 1992.
[22] F. Plestan, Y. Shtessel, V. Bregeault, A. Poznyak, New methodologies for adaptive sliding mode control, International journal of control 83 (9) (2010) 1907–1919.
[23] K. Ouari, T. Rekioua, M. Ouhrouche, Real time simulation of nonlinear generalized predictive control for wind energy conversion system with nonlinear observer, ISA transactions 53 (1) (2014) 76–84.